NOAA Technical Memorandum NWS TDL 70

THE SEA LEVEL PRESSURE PREDICTION MODEL OF THE LOCAL AFOS MOS PROGRAM

Techniques Development Laboratory
Silver Spring, Md.
April 1982

U.S. DEPARTMENT OF COMMERCE / National Oceanic and Atmospheric Administration / National Weather Service

NOAA Technical Memorandum NWS TDL 70

THE SEA LEVEL PRESSURE PREDICTION MODEL OF THE LOCAL AFOS MOS PROGRAM

David A. Unger

Techniques Development Laboratory
Silver Spring, Md.
April 1982

UNITED STATES
DEPARTMENT OF COMMERCE
Malcolm Baldrige, Secretary

National Oceanic and
Atmospheric Administration
John V. Byrne, Administrator

National Weather
Service
Richard E. Hallgren, Director

Table of Contents

		Page
	Abstract	1
1.	Introduction	1
2.	Prediction Methods of the SLP Model	3
	A. Prediction Equations	3
	B. Numerical Methods	4
	C. Sample Predictions and Verification Procedure	5
3.	Adjustments to the Model	8
	A. Recurring Errors	8
	B. Terrain Adjustments	8
	C. Advecting Winds	9
	D. Altimeter Setting Forecasts	10
4.	Results	11
	A. Verification Scores Over the Total Forecast Area	11
	B. Verification Scores by Region	12
	C. Effects of Smoothing on Forecasts	12
	D. Forecast Quality	13
5.	Conclusions	14
	References	14
	Appendix	16
	Table	17
	Figures	18

THE SEA LEVEL PRESSURE PREDICTION MODEL OF THE LOCAL AFOS MOS PROGRAM

David A. Unger

ABSTRACT. The Automation of Field Operations and Services (AFOS) project will eventually enable objective guidance such as Model Output Statistics (MOS) to be produced locally. Simple numerical models have been selected as part of the Local AFOS MOS Program (LAMP) to be run at weather service field offices to aid in the production of local MOS forecasts.

The sea level pressure (SLP) model which ran operationally at the National Meteorological Center (NMC) in the late 1960`s as a part of the Subsynoptic Advection Model (SAM) has been adapted for LAMP. The SLP model, with the changes that have been made from its original formulation, is documented here. The model predicts 1000-mb heights with an equation based on the principle of conservation of potential vorticity. The 1000-mb heights are estimated from hourly observations of sea level pressure, which enables the SLP model to be run at any hour with input from surface observation and a 500-mb height forecast from NMC`s LFM model. The model can be run on minicomputers similar to those used in AFOS, enabling guidance to be produced at local forecast offices.

Observations from 0800 GMT are used to test the SLP model`s ability to update the LFM forecast from 0000 GMT. Results from 30 sample winter cases and 15 summer cases indicate that the SLP model has more skill than the LFM for about 14 hours after 0800 GMT. Greater detail and more accurate placement due to the later initial data account for the more accurate predictions.

1. INTRODUCTION

The National Weather Service`s Automation of Field Operations and Services (AFOS) project will provide the field forecaster with on-station computer capabilities and enable rapid communication with other offices. The Data General Eclipse minicomputers placed at weather service field offices will be linked through a communications network, making local processing of meteorological data possible. It may soon be possible to run simple numerical models on this or similar equipment, enabling objective guidance to be produced locally.

A project under development at the Techniques Development Laboratory (TDL) to provide such objective products is the Local AFOS MOS Program (LAMP) (Glahn, 1980). This project involves running simple numerical models regionally to provide forecasts which can be used to update centrally produced Model Output Statistics (MOS) (Glahn and Lowry, 1972a) guidance. The model can be initialized with the most recent hourly data and in more detail than is used for the large-scale, centrally-run numerical models.

Since the models will most likely be run on a minicomputer, the amount of computations, Input-Output, and core storage required must be kept to a minimum. In addition, these models will be used to update forecasts at any hour, so only information available from hourly observations can be used. Transmission of large amounts of data in the form of numerical fields from the National Meteorological Center's (NMC's) models may prove taxing to the AFOS communications network and should be avoided.

The models selected for this project were adapted from a system known as the Subsynoptic Advection Model (SAM) (Glahn and Lowry, 1972b) which ran operationally at NMC from 1968 to 1973. It consisted of a sea level pressure (SLP) model developed by Reed (1963) and the SLYH moisture model, named from the last initials of its developers Frederick Sanders, Jerrold LaRue, Russell Younkin, and John Hovermale (Younkin et al., 1965). These models were driven by output from NMC's PE model (Shuman and Hovermale, 1968) and initialized with data derived from the most recent surface observations.

Simple advection models are also being developed to include in LAMP. They use winds derived from the output of the SLP model, and 500-mb height forecasts from NMC's LFM model (Gerrity, 1977) to advect fields such as precipitation type, ceiling, visibility, and sky cover. Forecasts of those elements can be used with the output from the SLP and SLYH models to derive MOS equations.

These models can be run on an Eclipse minicomputer and are capable of producing useful short range forecasts. They use data obtainable from hourly observations, making them suitable for updating existing guidance. They can be run locally at National Weather Service field offices over a regional grid.

This paper reports on the SLP model and some of the experiments that have been run in an attempt to improve its forecasts. Comparisons between the SLP and LFM predictions have been included to illustrate the advantage gained by the use of more detailed and recent initial data, and how long this advantage can be maintained.

2. PREDICTION METHODS OF THE SLP MODEL

A. Prediction Equations

The sea level pressure model is based on one developed by Reed (1963). It uses a potential vorticity equation at 1000 mb with an upper level forecast provided by a driving model. The 1000-mb heights are adjusted to conserve potential vorticity along a trajectory determined by an equivalent advecting wind (Fjortoft, 1952) computed from a smoothed 500-mb geostrophic flow and a terrain field. The 1000-mb heights are estimated from hourly observations of sea level pressure from the simple linear relation shown in Eq. (1).

$$Z_o = \frac{(P - 1000)}{.12015} \tag{1}$$

where Z_o is the 1000-mb height in meters, and P is the sea level pressure in millibars. Because of this very simple relationship, the Reed model is usually referred to as a sea level pressure model.

Once the initial 1000-mb height has been obtained, the SLP model uses a relationship derived from the potential vorticity equation shown in Eq. (2) to predict future states.

$$\frac{\partial(\zeta_o + f)}{\partial t} = - \vec{V}_o \cdot \nabla(\zeta_o + f) + (\zeta_o + f)\left(\frac{\partial \omega}{\partial p}\right)_o \tag{2}$$

The subscript "o" denotes values which are evaluated at the 1000-mb surface. ζ refers to the vorticity, f is the coriolis parameter, $\vec{V}$ is a horizontal advecting wind, p is pressure, and ω is the vertical motion.

By applying simplifying assumptions and extensive approximations, Eq. (2) becomes Eq. (3).

$$Z_o^{fd} = (Z_o - bZ_5 + M - G)^{iu} - (- bZ_5 + M - G)^{fd} \tag{3}$$

Here, Z_5 is the 500-mb height, M is a terrain term, G is a term which depends on latitude, and b is a constant. The superscript "iu" indicates the term is to be evaluated at the initial upstream end of a trajectory, while the superscript "fd" refers to the values at the forecast downstream end of the trajectory. Derivation of this equation can be found in Reed (1963) or Glahn and Lowry (1972b).

The trajectory is calculated from an equivalent advecting wind defined by the 500-mb height field and a terrain field as shown in Eq. (4).

$$\vec{V}_E = \vec{k} \times \frac{g}{f_{45}} \nabla(b\,\bar{Z}_5 - M) \qquad (4)$$

$\vec{V}_E$ is the vector advecting wind, f_{45} is the coriolis parameter at 45° latitude, g is the acceleration due to gravity, and $\bar{Z}_5$ is a smoothed 500-mb height field.

These equations were derived by assuming geostrophic approximations to vorticity and advecting wind, and approximations to the second derivative of Z_o to avoid obtaining Z_o from the 1000-mb vorticity by relaxation. A parabolic vertical velocity profile between the surface and 500-mb was also assumed in deriving Eq. (3).

Reed defined the terms in Eqs. (4) and (5) as follows:

$b = .55$;
$M = a\,PG$, where a is a constant set at .405 ($\frac{m}{mb}$) and PG is the average surface pressure in mb; and
$G = c \sin^2\phi$, where c is a constant equal to 163 m, and ϕ is the latitude.

The model was tuned in an attempt to improve the forecasts. The solutions were quite insensitive to the latitude term, so it was kept at the value given by Reed. The terrain term was treated separately in Eqs. (3) and (4), as was the factor b multiplying the 500-mb heights.

Eqs. (3) and (4) can then be rewritten as

$$Z_o^{fd} = Z_o^{iu} - b_1(Z_5^{iu} - Z_5^{fd}) + a_1(PG^{iu} - PG^{fd}) - c(\sin^2\phi^{iu} - \sin^2\phi^{fd})$$

(a) (b) (c) (d) (5)

$$\vec{V}_E = \vec{k} \times \frac{g}{f_{45}} \nabla(b_2\bar{Z}_5 + a_2\,PG) \qquad (6)$$

Eq. (5) states that the predicted 1000-mb heights are determined by advection (term a), with development along the trajectory induced by changes in the 500-mb height (term b), terrain (term c), and latitude (term d).

B. Numerical Methods

A Lagrangian technique is used in the solution of Eq. (5), with trajectories computed from Eq. (6). Fig. 1 shows the grid on which these equations are solved (the computational grid). The grid spacing is shown

in the lower left hand corner by the points, with circles indicating points where the LFM heights are available. A 1-h timestep is used in the solution.

When it was a part of SAM, the SLP model obtained Z_5 from the PE model. The field was available on a one Bedient[1] grid and was smoothed with a 25 point smoother which was often used in SAM. The smoothed value at each point was simply an average of all values within a box 5 gridpoints on a side centered at the point.

Presently, the 500-mb heights are available each 6 hours from archived LFM forecasts. They are interpolated in time by fitting a cubic polynomial by least squares to the seven LFM forecasts for hours 0, 6, ..., 36 at every gridpoint to obtain values at each hour. $\overline{Z}_5$ is obtained by applying a smoother to this field. Experiments indicate that smoothing over the same area as in SAM produced the best predictions. Since LFM data are available on a one-half Bedient grid, this involves smoothing over a box 9 gridpoints on a side. Both Z_5 and $\overline{Z}_5$ are then interpolated bi-linearly to the one-quarter Bedient grid used in the SLP model.

The geostrophic winds are calculated from $\overline{Z}_5$. These winds are used in constructing trajectories ending over the gridpoints after each timestep. Upstream quantities used in Eq. (5) are obtained by interpolating the initial values bi-linearly to the trajectory origins. Downstream conditions are taken from the gridpoint values the following hour.

C. Sample Predictions and Verification Procedure

Although the SLP model will eventually be run locally, testing of the model and developing MOS equations requires NOAA`s large computers. For testing, the forecast area includes the entire United States rather than regional sections to be used when the SLP model is run locally.

Analysis maps are obtained from hourly observations by a Cressman type objective analysis similar to that used in SAM (Glahn et al., 1969). Sea level pressure reports are processed to produce an analyzed field on the computational grid.

---

[1] A Bedient refers to the grid spacing associated with a polar stereographic projection true at 60°N which was used with NMC`s early models. At 60°N 1 Bedient is equal to 381 km.

The model was tuned with 16 cases from January through March 1979 and 14 cases from the summer of 1979. Fourteen cases from the winter of 1977-1978 were selected as independent data. Some of the cases were selected at random, while others were chosen to examine the model`s handling of systems in particular regions of the country.

Verification scores used to test the accuracy of the SLP forecasts are the S1 score (Teweles and Wobus, 1954), the mean absolute error (MAE), and the mean error. Scores are computed on a one-half Bedient grid, which coincides with the grid on which LFM data are available and coincides with alternate grid points on the SLP model`s computational grid. All scores are computed from 1000-mb height values.

The S1 score is computed in the same manner as at NMC. The score is a measure of the accuracy of the gradient forecasts and is independent of the mean error. A low score represents a better forecast, with scores below 30 generally regarded as highly accurate, and those above 80 regarded as valueless (Badner, 1966).

The (MAE) measures the overall magnitude of errors. It is not entirely reliable as an indicator of the pressure pattern forecast; however, it does indicate how close the predicted 1000-mb heights are to the observed ones.

The mean error measures the overall bias of the 1000-mb height forecast. It is the average difference between forecast and observed (forecast minus observed) values of Z_o over all verification gridpoints.

Forecasts are verified over the area outlined by the dark solid line in Fig. 1. Three sub-regions have been defined as shown by the dashed lines to study the model`s behavior by section of the country. The western region includes the Pacific Ocean and mountainous areas, the central region includes the plains states, and the east coast region includes the eastern states. It was found that the model behaves similarly in the east coast and the central regions. Therefore, results displayed in this report are computed by combining these two into one region named the eastern region.

Results express errors in terms of differences between the 1000-mb heights predicted from the SLP model and those determined from sea level pressure analysis and Eq. (1). The MAE and mean error are measured in meters and can be converted to sea level pressure errors in millibars by multiplying by .12015.

In the past, SAM was run with 0700 GMT data to produce guidance in time for the early morning forecast. On AFOS, 0800 GMT observations can prob-

ably be processed in time for the early morning forecast, so 0800 GMT has been chosen as one initial time on which to test the LAMP system.

Verification statistics presented here are based on SLP forecasts initialized at 0800 GMT and compared to those of the LFM 1000-mb forecasts initialized at 0000 GMT. Standard 6-h intervals for which the LFM forecasts are available have been chosen for verification, so a 4-h projection for the SLP model is compared to the 12-h LFM forecast valid at 1200 GMT. Simarly, the 10-, 16-, and 22-h projections will be compared to the 18-, 24-, and 30-h LFM forecasts valid at 1800, 0000, and 0600 GMT respectively. These comparisons are illustrated in Fig. 2.

Considerable attention was devoted to smoothing the SLP forecasts. Since the S1 score is sensitive to the positioning of gradients, small scale detail must be placed accurately in order to maintain good scores. Meaningless detail can result in a considerable worsening of the S1 scores. Although the Lagrangian solutions tend to smooth fields through interpolations, additional smoothing improves the S1 score and, to a lesser extent, the MAE. Only output fields are smoothed, since detail is permanently lost if smoothing is included as part of the prediction process.

Most scores presented here are from output smoothed by the 25 point smoother on the computational grid. By reducing the noise, smoothing places emphasis on the synoptic patterns in the verification scores. In addition, the SLP model overpredicts the pressure gradients. Smoothing the forecasts aids in reducing the gradients, and therefore improves the forecast quality.

Persistence forecasts were also compared to the SLP predictions. As will be discussed in a later section, detail in the initial analysis is often the result of orographic influence in obtaining sea level pressure from surface pressure. This detail causes unsmoothed persistence forecasts to score better in the S1 score than those which are smoothed. Since the accuracy of the persistence forecast is greater without smoothing, the initial analysis maps are used directly as persistence forecasts.

The LFM forecasts are already quite smooth, and additional smoothing made no significant difference in verification scores. The 1000-mb heights have been estimated from Eq. (1) and the LFM sea level pressure forecast. LFM sea level pressure forecasts score slightly, but consistently better than the LFM 1000-mb height predictions, averaging about .5 lower in the S1 score and about 1.0 m lower in the MAE. The sea level pressure forecasts from the LFM have been archived at 12-h intervals while 1000-mb height forecasts are available every 6 hours. Since the difference in accuracy of the two forecasts is not great, the information

gained through the greater availability of the LFM 1000-mb forecasts justifies their use for comparison with the SLP model.

3. ADJUSTMENTS TO THE MODEL

A. Recurring Errors

The SLP model has been tuned in an attempt to control certain undesirable features. Some notable shortcomings of the original SLP model are:

1. Overbuilding of high pressure systems and a slight overdeepening of lows.

2. A tendency to develop tear-drop shaped highs. This occurs when high pressure builds too rapidly in regions to the south and southwest of well developed cyclones.

3. Southeast extensions are what Reed referred to as the SLP model`s tendency to develop anomalous low pressure to the southeast of cyclones, giving them a northwest-southeast tilt.

4. Distorted features in mountainous regions such as hooks of high or low pressure and strong gradients.

Adjustments have been made in an attempt to eliminate these errors. Although changes have resulted in improvements, these errors have not been entirely eliminated.

B. Terrain Adjustments

Since the model predicts the pressure over the Rocky Mountains, the terrain term was carefully examined. Mountains influence both the steering (Eq. (6)) and development of systems (term c in Eq. (5)).

Reducing the weight of the terrain in the development term is accomplished by lowering the value of the constant, a_1, in Eq. (5). This improves the predictions until a_1 is about one-half of the value used by Reed, beyond which further reduction results in a slight worsening of the forecasts. With the reduced mountain term, the forecasts appear smoother; however, the effect of the terrain on the development is small when compared to advection. Therefore, the constant a_1 is set to one-half the value used by Reed (a_1 = .203).

The terrain term influenced the steering of systems (Eq. (6)) more than it influenced the development (Eq. (5)). Any reduction of a_2 in Eq. (6) resulted in systems moving eastward too rapidly in the plains

states and along the west coast. The terrain term gives a southerly component to trajectories just east of the Rocky Mountains, and a northerly component to systems off the west coast. It enhances the southerly push of high pressure into the Texas-Oklahoma region and aids the development of the lee of the mountain trough. This behavior is commonly observed in nature and is often of considerable importance to the weather of these regions.

Unfortunately, a large terrain term creates strong gradients and unrealistic features in the mountains, a problem which has been attributed to strong orographically induced convergence. Orographic detail tends to create fictitious features in rough terrain. As a result, the model terrain height was selectively reduced in the Rocky Mountains while retaining its full value elsewhere. This was accomplished by reducing the terrain with the logarithic function discussed in the Appendix. This filter is applied at elevations above an empirically determined value selected to give the greatest improvement in the mountains without worsening forecasts in the central region of the country.

C. Advecting Winds

Another important parameter in the SLP model is the advecting wind speed. Former empirical studies have shown that surface systems move nearly parallel to and at 50 to 60 percent of the 500-mb geostrophic wind speed (Riehl et al., 1952).

The SLP model does not directly use 500-mb heights for computing winds, but uses a heavily smoothed 500-mb height forecast from the LFM. Choosing the proper speed with which to advect surface systems is further complicated by the tendency of some parts of the system to move systematically faster or slower than others relative to the 500-mb winds. For instance, the model characteristically moves low pressure centers slightly slower than is observed, while fronts trailing from well developed lows are often moved faster than observed when Reed's value of 55 percent of the 500-mb geostrophic flow was used for advection in Eq. (6) ($b_2 = .55$).

For winter cases, predictions made with b_2 about 30 percent lower than the .55 used by Reed resulted in the lowest S1 scores. Visual inspection of these forecasts made with the lower constant revealed that systems were moving too slowly in the east and central United States, with improvement mainly coming from the western states. Since the speed of movement is very important for short range forecasting, the S1 score is not entirely reliable as an indicator of the forecast quality. Some pressure patterns are the result of stationary features created by the terrain (for example, cold air damming by mountain ridges can create sharp pressure

gradients). This can cause the S1 score to be better for lower advection rates than it would if only migrating pressure systems were considered. Since the advection of synoptic weather patterns is of more interest than local effects in this work, b_2 was selected to give accurate movement. It was found that best results were obtained with $b_2 = .55$.

In summer cases, the model also produced best results with $b_2 = .55$, when both of S1 score and the movement of systems were considered. At this time of year, systematic differences in advection rates in different parts of a synoptic system are much less pronounced.

Although the problem of too rapid movement of surface systems in regions of strong 500-mb winds could not be eliminated without producing slow forecasts elsewhere, one approach which seemed to give some improvement was to decrease some of the higher 500-mb winds.

The filter used to lower winds is shown in the Appendix. It is only applied to winds above 41 kt as computed from the smoothed LFM 500-mb heights. This cutoff was chosen by observation of the distribution of wind speeds at gridpoints for good and bad forecasts. When wind distributions for the six best and six worst forecasts as measured by the S1 scores from 16 winter cases were examined, it was found that poor forecasts had more gridpoints with high equivalent advecting winds. There were, for instance, twice as many gridpoints with winds greater than 55 kt for the six poor forecasts as for the good forecasts. The discrepancy involved the greatest number of points at the chosen cutoff.

D. Altimeter Setting Forecasts

One unsuccessful attempt at improving the SLP forecasts was to try altimeter setting to estimate the initial and verifying 1000-mb heights. There are about 30 percent additional stations reporting altimeter setting each hour than report sea level pressure. The SLP model was tested with this field in order to determine the advantages of having a more detailed initial analysis.

Results displayed in Fig. 3 reveal that use of the more detailed data increased the S1 score; although not shown, the MAE also increased. This is to be expected, since there is simply more small scale detail present, and the lower scores do not necessarily reflect a less accurate forecast.

To account for the effect of additional data, forecasts were compared to persistence. Persistence of altimeter setting performed better, relative to altimeter setting based forecasts, than did the sea level pressure persistence forecasts when they were compared to sea level pressure forecasts. This can be seen by observing the differences

between the forecast scores and the associated persistence score in Fig. 3. At no time is the improvement over persistence for the altimeter setting based forecasts (dashed lines) greater than the improvement of sea level pressure forecasts made over the sea level pressure persistence forecasts (solid lines). This indicates that the sea level pressure forecasts are of more value in predicting changes.

In addition, use of altimeter setting would greatly complicate obtaining accurate thickness forecasts from the 1000-mb heights of the SLP model, since the sea level pressure reduction formula contains information on the station temperature and the altimeter setting formula does not. Because thickness forecasts are a crucial element in LAMP, use of altimeter setting in the development of the model has been abandoned.

4. RESULTS

A. Verification Scores Over the Total Forecast Area

There were no significant differences between verification statistics for the independent and dependent sample, so verification results from both data sets were combined to give winter statistics. Figs. 4-6 compare the S1 score, MAE, and mean error of the SLP, LFM, and persistence forecasts for the 30 winter cases. These results indicate, as expected, that the SLP model derives its advantage over the LFM foreasts through more detailed and recent initial analysis, since its scores decay at a rate which is always greater than the LFM`s.

When considering the entire archive area (Fig. 4), persistence forecasts show the best S1 scores up to about 8 hours, with the SLP model best from 8 to 14 hours, and the LFM best beyond that. Therefore, 1000-mb height patterns obtained from the SLP model forecasts initialized at 0800 GMT will, on the average, be more accurate than the LFM`s through 2200 GMT.

The 1000-mb height forecasts from the SLP model show the lowest MAE for the entire 22-h forecast period. The persistence MAE is better than the MAE of the LFM for 9 hours, although it rapidly deteriorates throughout the forecast (see Fig. 5).

The mean errors are shown in Fig. 6. This score is equivalent to the difference in mean height between the forecast and analysis maps. The similarity in mean error of the SLP model and persistence forecasts indicate that the SLP model does not significantly change the mean 1000-mb height over the forecast area. Although on individual forecasts development of pressure systems can result in considerable bias, when many forecasts are combined the mean error averages to near zero with the

remaining bias due mostly to the failure of the SLP model to detect the normal diurnal pressure variation.

Summer results are presented in Figs. 7-9 and show essentially the same relationship between the LFM and SLP model as do the winter results. Even though the rate of decay of the SLP model`s S1 scores is greater in summer, the scores are still better than those produced by the LFM until about 14 hours after 0800 GMT. The summertime MAE for the SLP model is better than either persistence or the LFM throughout the 22-h forecast, as was observed in the winter cases. Relative to the SLP and LFM models, persistence S1 scores and MAE are better in the summer indicating an increased importance of local effects and generally weaker synoptic patterns.

B. Verification Scores By Region

Verification scores have been computed by region to provide further insight into the SLP forecasts. Fig. 10 shows the S1 score and MAE in the western and eastern regions. The S1 scores for persistence forecasts are better than those for the SLP or LFM predictions in the western region for the entire 22-h forecast, while in the eastern region the SLP model always scores better than persistence. The MAE`s for persistence forecasts are worse than the SLP model`s throughout the forecast in both regions.

Summer scores show similar patterns except that persistence performs better on both scores relative to its winter performance (see Fig. 11). A diurnal effect is evident by the improvement in S1 scores and MAE`s between 16 and 22 hours. Both the SLP and LFM models perform poorly in the western region.

C. Effect of Smoothing on Forecasts

Table 1 shows the effect of smoothing on the S1 scores and the MAE. Forecasts were smoothed with the 25 point smoother described earlier. As can be seen, while smoothing the 4-h forecast has little effect on the SLP model, it considerably worsens the persistence forecasts. At 16 hours, the SLP forecasts are improved while persistence forecasts are worsened, leading to a 3.75 greater point difference in total area S1 scores between smoothed and unsmoothed forecasts. Most of this difference originates from the western section of the country. Summer patterns are similar and somewhat more pronounced.

Evidently, reducing station pressure to sea level over mountainous terrain and pockets of cold or warm air in the valleys and deserts of the west create a persistent background pattern superimposed on the synoptic

systems. The SLP model will move this pattern with the advecting wind, misplacing small scale detail which is accurately placed by the persistence forecast. Because the small scale patterns influence the S1 scores to a larger extent than the MAE`s, smoothing will have a greater impact on the S1 scores. Persistence forecasts have orographic detail present in the forecasts which can improve the S1 scores even after 22 hours.

D. Forecast Quality

Examination of some forecasts reveals how the quality of the SLP forecasts varies over the forecast period. At 4 hours, the unsmoothed SLP forecasts are difficult to distinguish from the verifying analyses, while the 12-h LFM forecast which verifies at the same time appears quite smooth.

By 10 hours, the SLP model begins to develop its peculiar characteristics. It is slightly smoother than the analysis, and rapidly moving systems begin to appear stretched, although SLP forecasts are still superior to the LFM forecasts in most cases.

By 16 hours, the SLP predictions are about the same or perhaps slightly worse than the LFM 1000-mb predictions in forecast quality. There are fewer distortions in the LFM forecasts, and many of the systems appear to be placed more accurately. The SLP model tends to increase the pressure gradients, making more intense features than are observed. Low pressure centers move slightly slow while trailing fronts often are moved correctly, or slightly fast in areas of strong upper level winds.

An example of a forecast in shown in Figs. 12-15. The initial map from March 10, 1979, at 0800 GMT is shown in Fig. 12, with the smoothed 16-h SLP model forecast valid at 0000 GMT March 11, 1979, shown in Fig. 13. The 24-h LFM forecast valid at the same time is shown in Fig. 14, and the verifying analysis in Fig. 15. This sample was chosen because of its fairly typical scores and sharply defined pressure systems.

The SLP model overbuilt the high pressure system in the plains, as did the LFM to a lesser extent. The pattern in the mountain states was not predicted particularly well by either model, although the SLP model scores are slightly better.

The eastern United States is well-predicted by both models. The LFM is very slightly fast; however, due to its better placement of the high, it`s S1 score is slightly better.

The S1 score for the SLP model`s forecast is 60.2 over the total verification region, with a score of 67.4 in the western region and 52.2 in the eastern region. The LFM scores for the total, western, and

eastern regions are 57.2, 68.3, and 51.9 respectively. The overall MAE is 19.0 meters for the SLP model and 20.4 meters for the LFM.

5. CONCLUSIONS

The SLP forecasts were evaluated on 30 winter and 14 summer cases. These were compared to LFM forecasts produced 8 hours earlier in order to test the value of the updated predictions. Results indicate that the SLP model produces forecasts which are more accurate than the LFM for about 14 hours, meaning that useful improvement can be obtained until about 2200 GMT when initialized at 0800 GMT. Therefore, the SLP model may produce better 1000-mb forecasts for most of what is known as the "today" period.

The tests here indicate that procedures which depend on accurate sea level pressure forecasts should benefit from the SLP model update. The SLP model predicts for the central and eastern section of the country with greater accuracy than in mountains. It remains to be seen how the SLP model will aid in the prediction of variables such as thickness and contribute to the advecting wind for the moisture and advection models. Ultimately, the value of the SLP model will rest on its ability to provide information which can increase the accuracy of MOS forecasts when run locally on AFOS or similar equipment.

REFERENCES

Badner, J., 1966: Performance of the 6 layer baroclinic (primitive equation) model. ESSA Technical Memorandum WBTM-FCST-5, U.S. Weather Bureau, U.S. Department of Commerce, 68 pp.

Fjortoft, R., 1952: On a numerical method of integrating the barotropic vorticity equation. Tellus, 4, 179-194.

Gerrity, J. F. Jr., 1977: The LFM model-1976: A documentation. NOAA Technical Memorandum NWS NMC-60, National Oceanic and Atmospheric Administration, U.S. Department of Commerce, 68 pp.

Glahn, H. R., 1980: Plans for the development of a local AFOS MOS program (LAMP). Preprints Eighth Conference on Weather Forecasting and Analysis, Denver, Amer. Meteor. Soc., 302-305.

_____, G. W. Hollenbaugh, and D. A. Lowry, 1969: An operationally oriented objective analysis program. ESSA Technical Memorandum WBTM TDL 22, U.S. Weather Bureau, U.S. Department of Commerce, 20 pp.

_____, and D. A. Lowry, 1972a: The use of model output statistics (MOS) in objective weather forecasting. J. Appl. Meteor., 11, 1203-1211.

_____, and D. A. Lowry, 1972b: An operational subsynoptic advection model (SAM). J. Appl. Meteor., 11, 578-585.

Reed, R. J., 1963: Experiments in 1000-mb prognosis. NMC Technical Memorandum 26, U.S. Weather Bureau, U.S. Department of Commerce, 29 pp.

Riehl, H., J. Badner, J. E. Hovde, N. E. La Seur, L. L. Means, W. C. Palmer, M. J. Schroeder, and L. W. Snellman, 1952: Forecasting in middle latitudes. Meteorological Monographs, Amer. Meteor. Soc., 80 pp.

Shuman, F. G., and J. B. Hovermale, 1968: An operational six-layer primitive equation model. J. Appl. Meteor., 7, 525-547.

Teweles, S. Jr., and H. B. Wobus, 1954: Verification of prognostic charts. Bull. Amer. Meteor. Soc., 35, 455-463.

Younkin, R. J., J. A. LaRue, and F. Sanders, 1965: The objective prediction of clouds and precipitation using vertically integrated moisture and adiabatic motions. J. Appl. Meteor., 4, 3-17.

APPENDIX A

The Logarithmic Filter

High wind speeds and terrain heights are filtered with the logarithmic filter described below.

Without scaling considerations, the filter takes the form

$$A_F = C_1 \ln(A+C_2) + C_3 \qquad \text{for } A > A_{min}, \qquad (7)$$

where A is the unfiltered quantity, and A_F is the filtered value. C_1, C_2, and C_3 are constants which depend on the minimum value, A_{min}, for which filtering is desired.

Terrain above 1250 m is filtered by the equation,

$$M_F = 500 \ln(.02M-4.91)-250, \qquad \text{for } M > 1250 \text{ m} \qquad (8)$$

where M is the terrain height in meters. The filtering characteristics are shown in Fig. 16a.

Winds greater than 41 kt are filtered by Eq. (9).

$$V_F = 18.7 \ln(.531V-1.91)-14.96, \qquad V > 41 \text{ kt} \qquad (9)$$

where V is the magnitude of the geostrophic wind in knots as computed from the smoothed 500-mb heights from the LFM.

The filtering characteristics are shown in Fig. 16b.

Table 1. S1 Scores and MAE for smoothed and unsmoothed 1000-mb height forecasts for 12 cases from the 1978-79 winter season.

		S1 Score		MAE (m)	
		Unsmoothed	Smoothed	Unsmoothed	Smoothed
Total Area	4-h SLP Forecast	35.80	35.48	9.94	9.75
	4-h Persistence Forecast	33.52	36.55	12.30	12.48
	16-h SLP Forecasts	60.62	57.27	27.02	25.86
	16-h Persistence Forecast	67.27	67.68	38.02	37.27
Western Region	4-h SLP Forecast	45.50	45.25	10.18	9.91
	4-h Persistence Forecast	37.66	42.77	10.38	10.70
	16-h SLP Forecast	69.37	65.13	25.22	24.17
	16-h Persistence Forecast	65.23	67.31	29.67	29.00
Eastern Region	4-h SLP Forecast	34.04	34.16	8.81	8.63
	4-h Persistence Forecast	33.49	35.96	11.91	11.95
	16-h SLP Forecast	59.97	57.75	27.13	26.02
	16-h Persistence Forecast	70.59	70.71	39.04	38.31

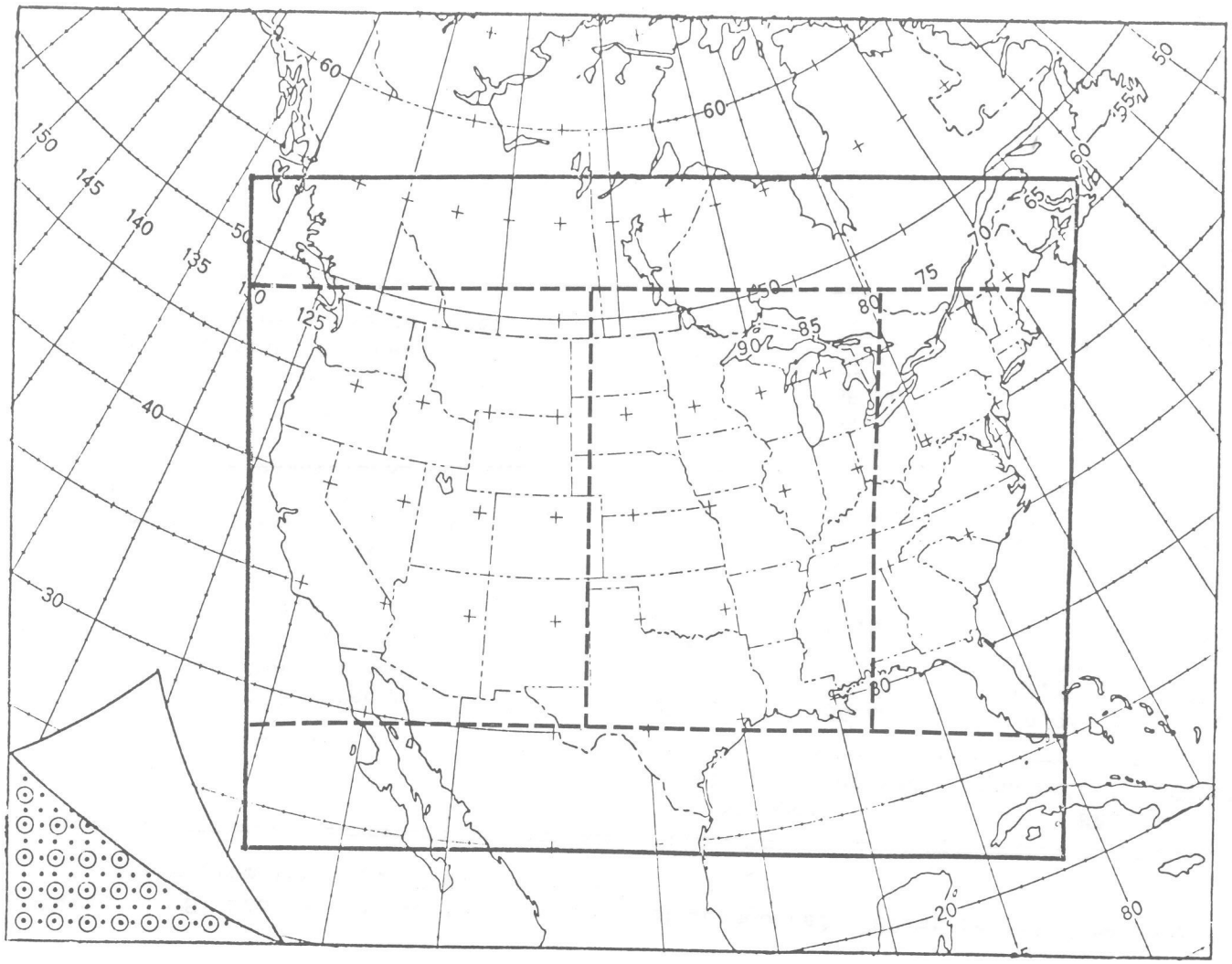

Figure 1. Area over which the SLP model is computed. The overall verification area is outlined by the solid line. The Western, Central, and East Coast Regions are shown by the area within the dashed lines. The grid spacing used by the SLP model is shown in the lower left, with circles indicating the grid on which LFM data are available.

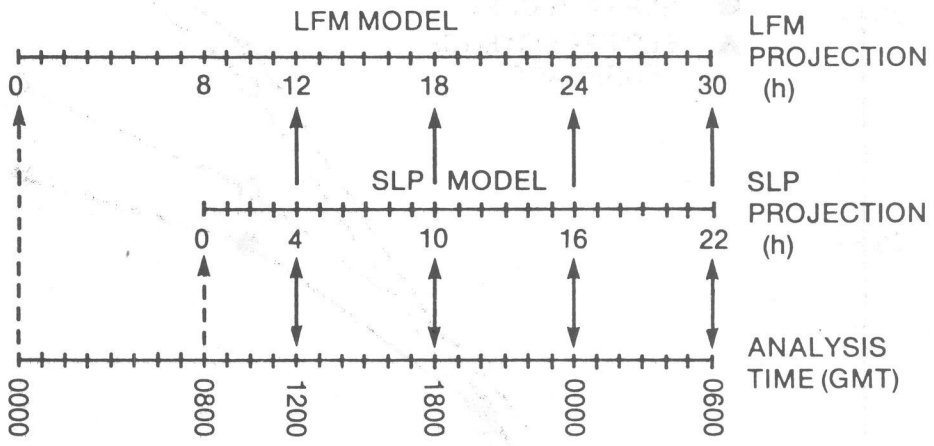

Figure 2. Relationship between initialization time, projection hour, and verification time between the LFM and SLP model. Dashed vertical lines indicated initialization times.

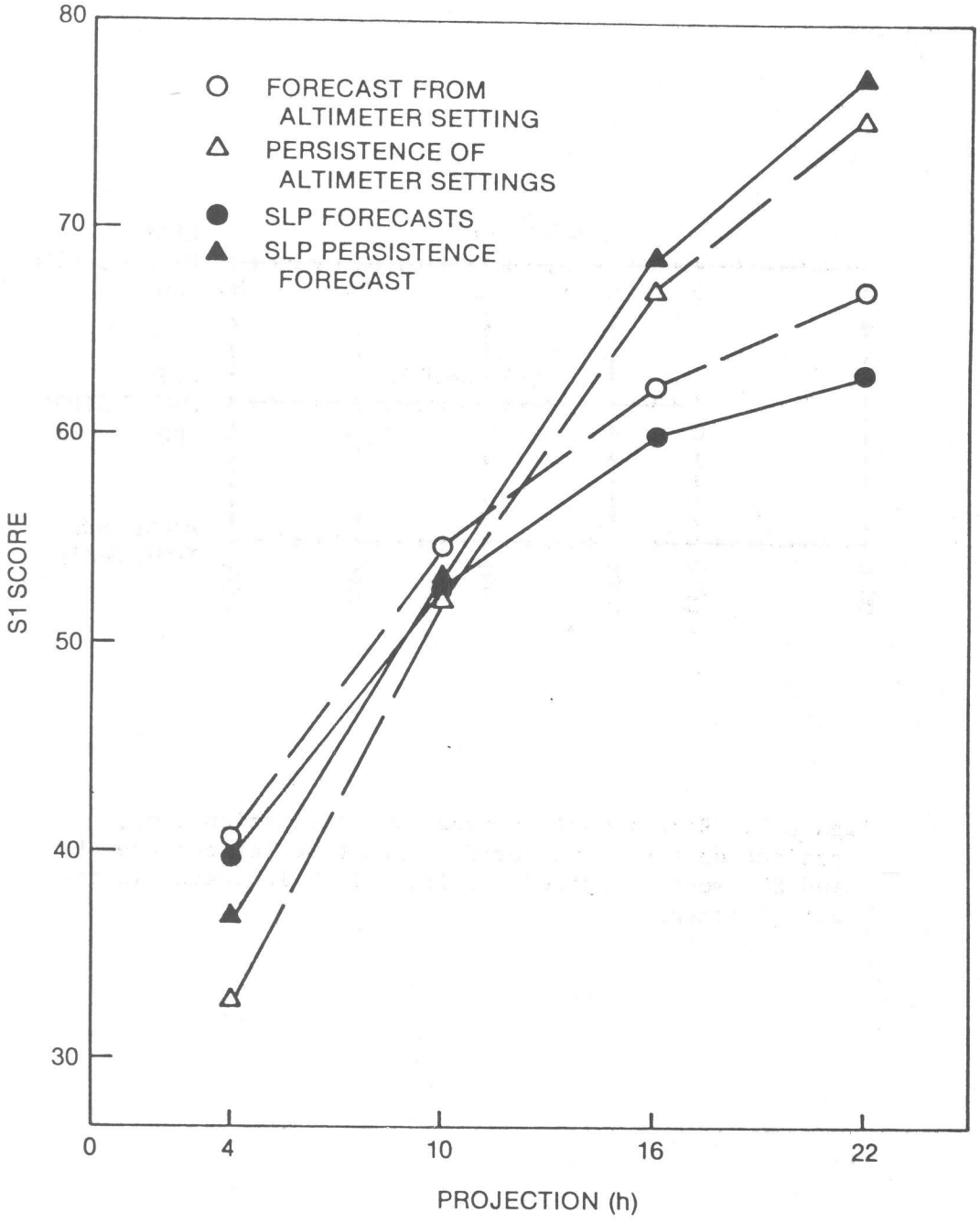

Figure 3. Average S1 scores from 16 winter forecasts of 1000-mb heights initially estimated from altimeter setting (dashed lines) and sea level pressure (solid lines). The associated persistence scores are also displayed.

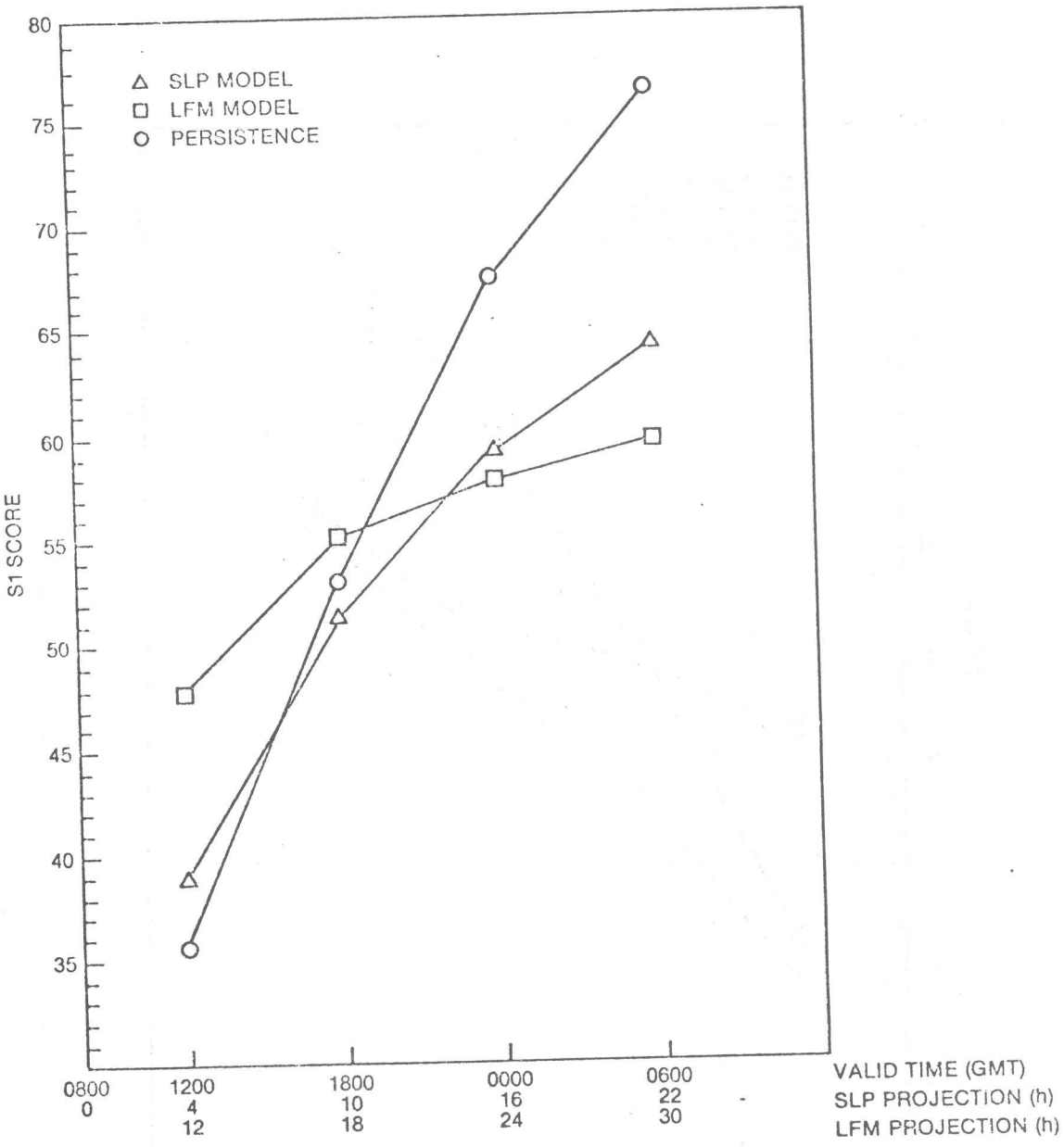

Figure 4. S1 scores over total verification region for SLP model and persistence 1000-mb height forecasts initialized at 0800 GMT and LFM forecasts initialized at 0000 GMT. S1 scores are from an average of 30 cases from winter 1977-78 and winter 1978-79.

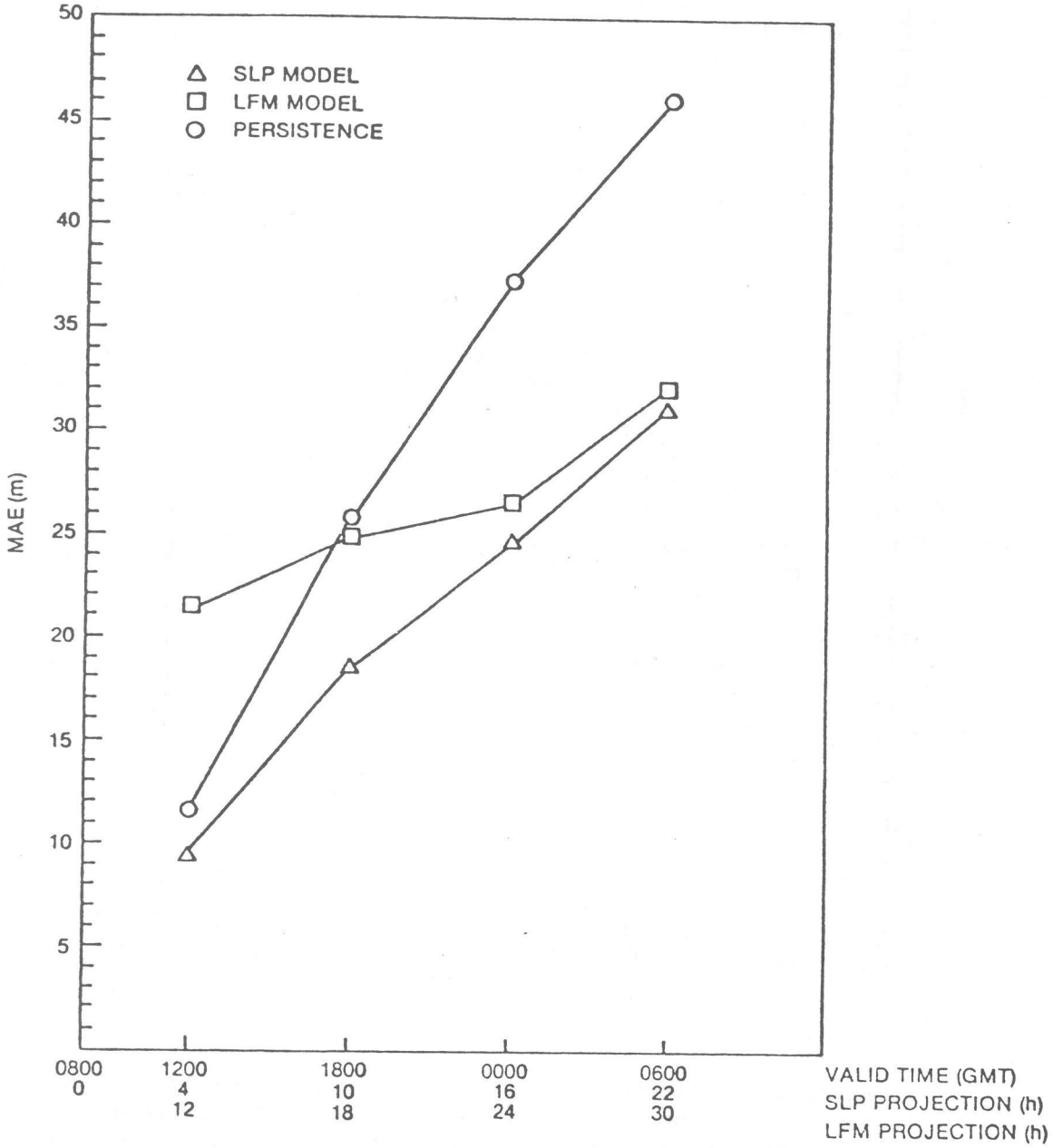

Figure 5. Same as Fig. 4 except for mean absolute error.

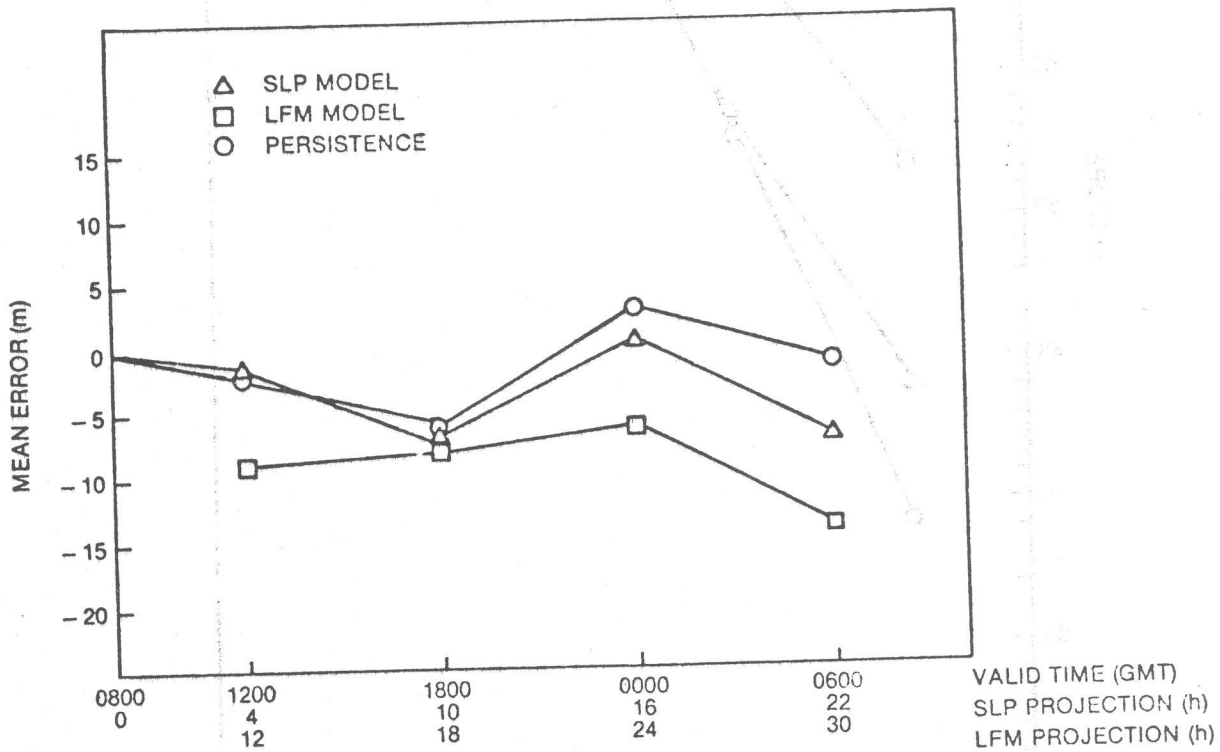

Figure 6. Same as Fig. 4 except for mean error.

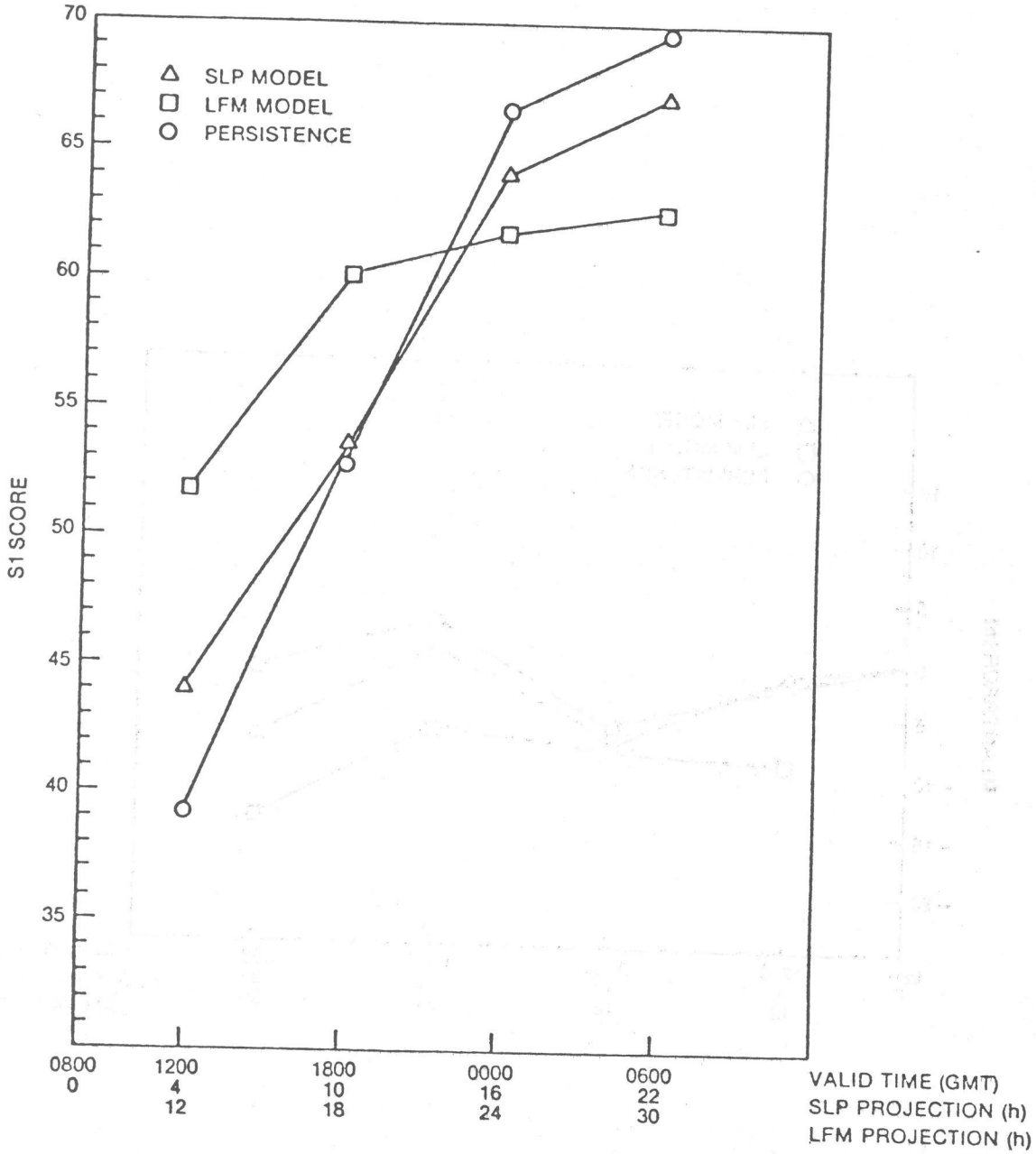

Figure 7. Same as Fig. 4 except averages of 14 summer cases.

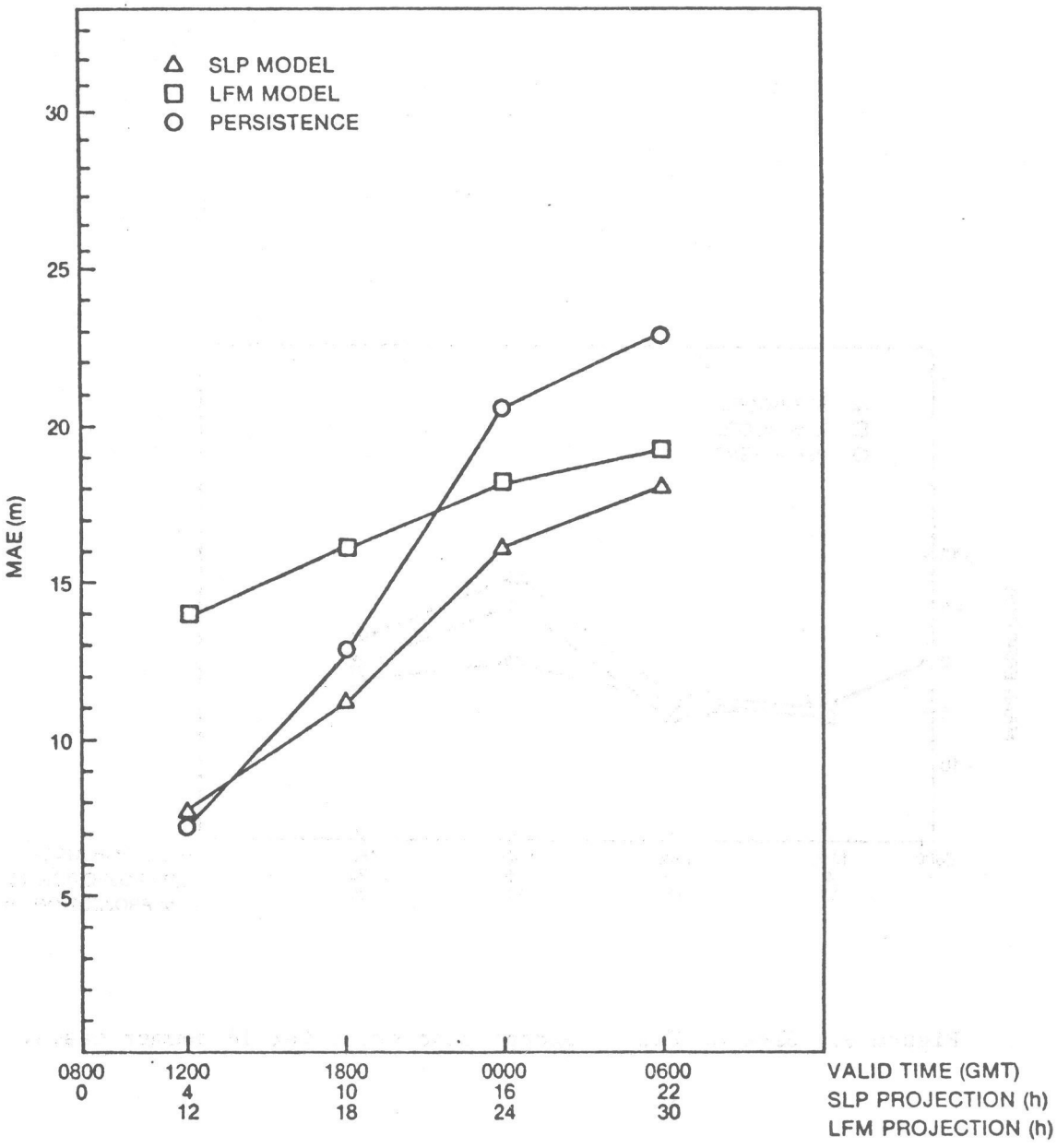

Figure 8. Same as Fig. 4 except mean absolute error for 14 summer cases.

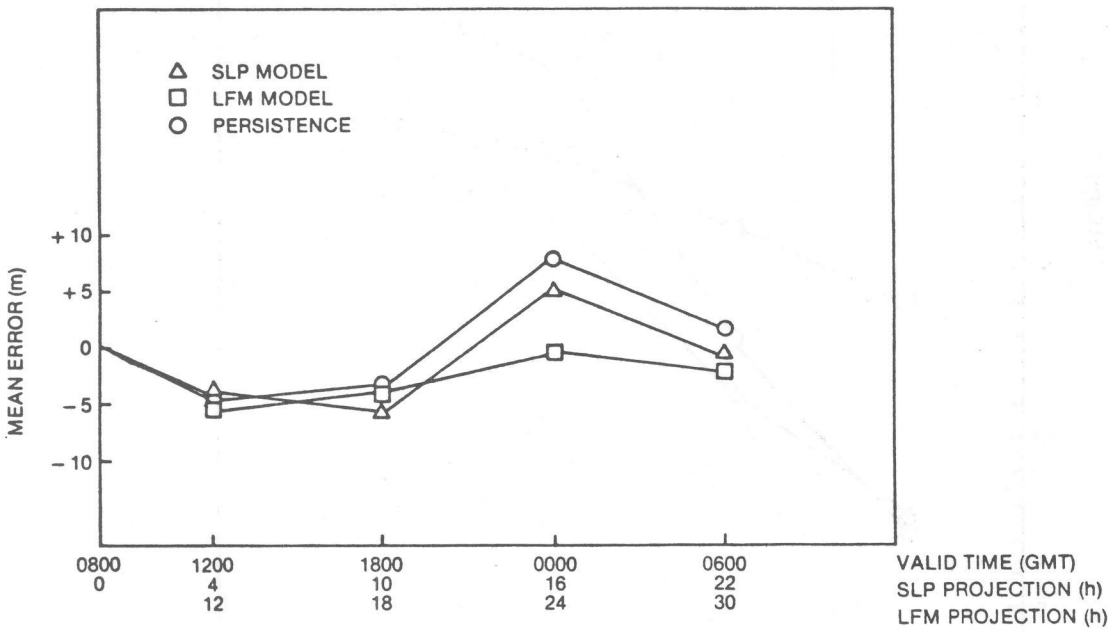

Figure 9. Same as Fig. 4 except mean error for 14 summer cases.

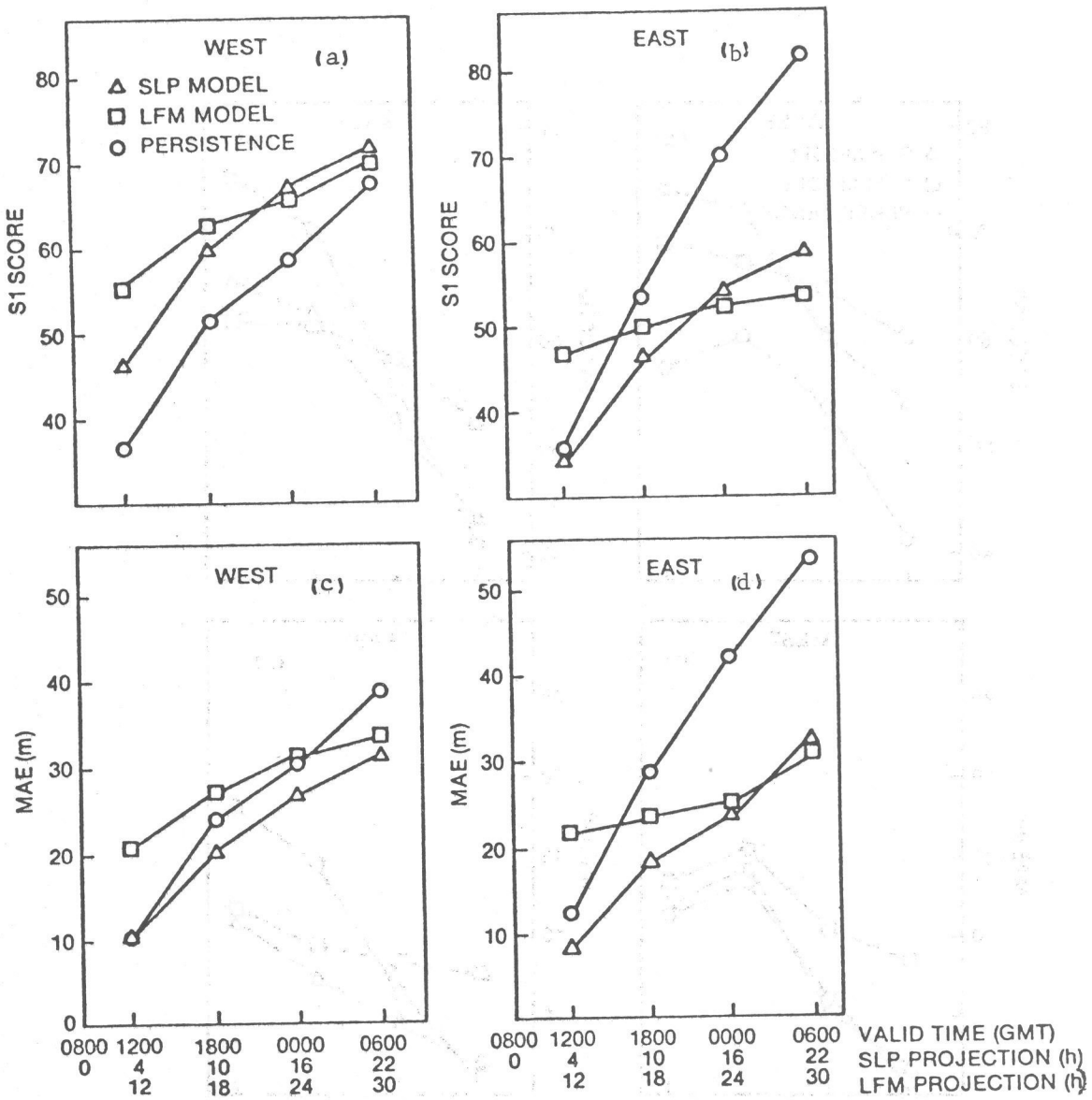

Figure 10. S1 scores for winter cases for SLP and persistence forecasts initialized at 0800 GMT and LFM forecasts initialized at 0000 GMT for various verifying times--for Western Region (a) and Eastern Region (b). Mean absolute errors for the same cases are shown for Western Region (c) and Eastern Region (d).

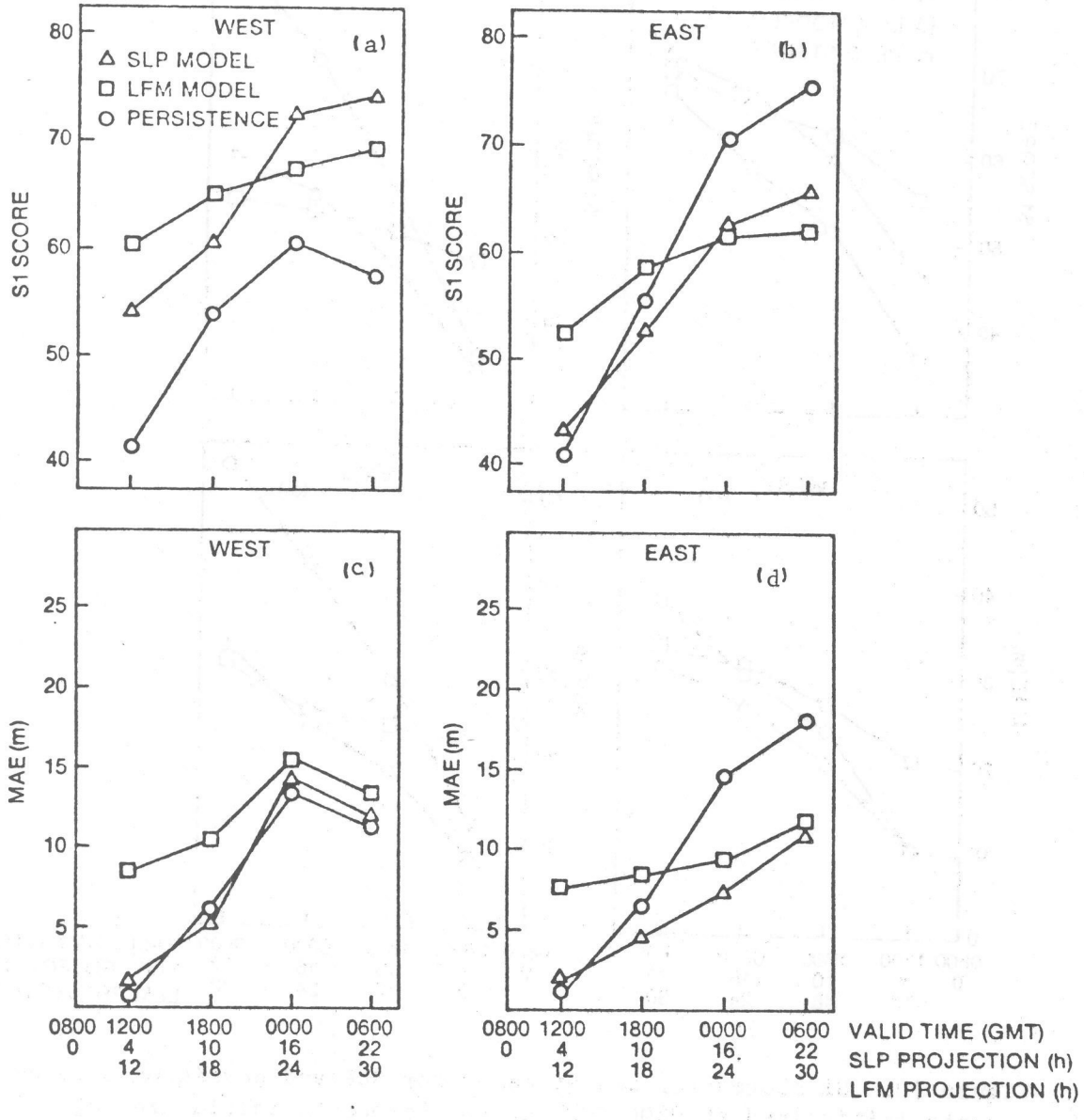

Figure 11. Same as Fig. 10 except for 14 summer cases.

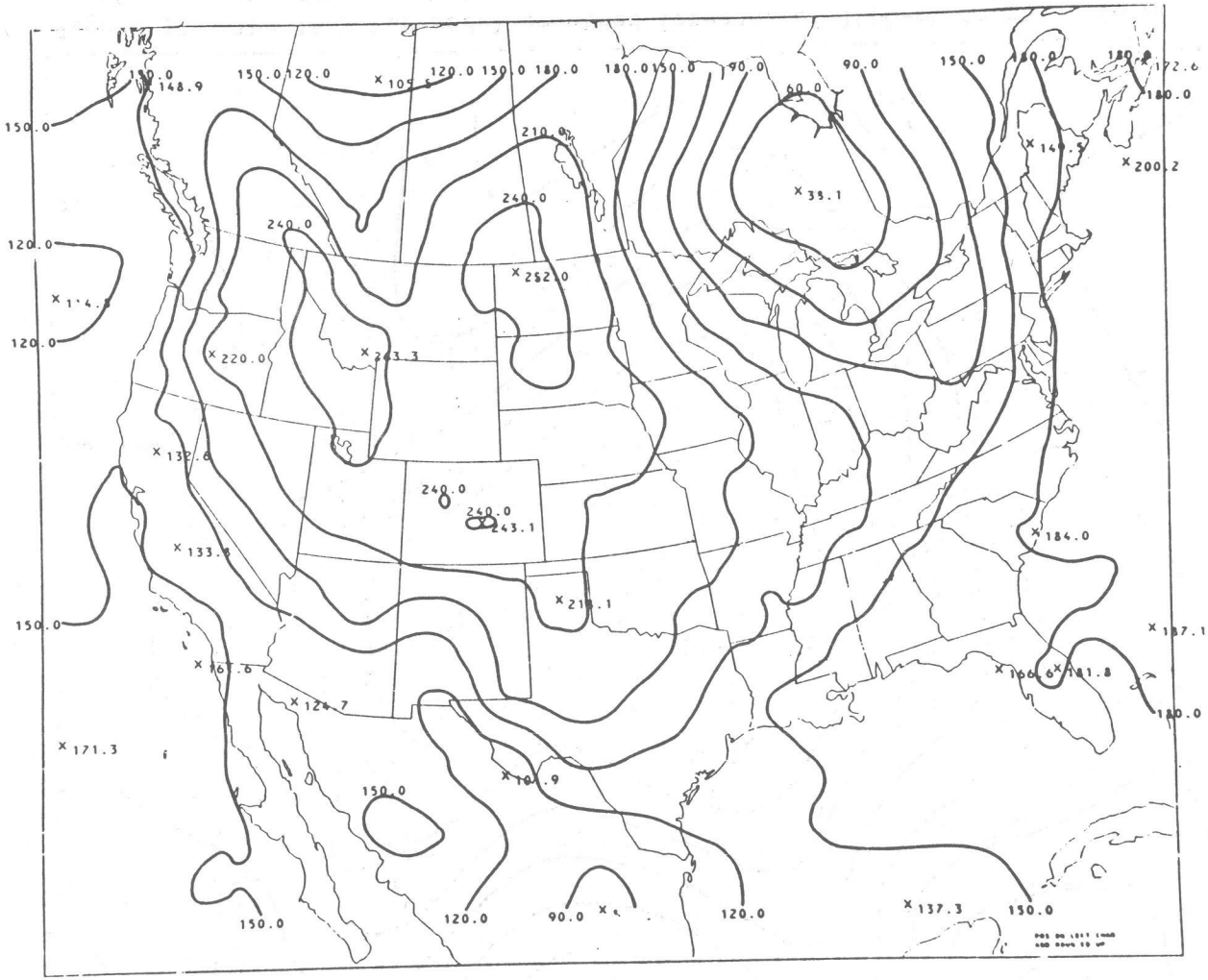

Figure 12. Initial analysis of 1000-mb heights, in meters, for 0800 GMT, March 10, 1979.

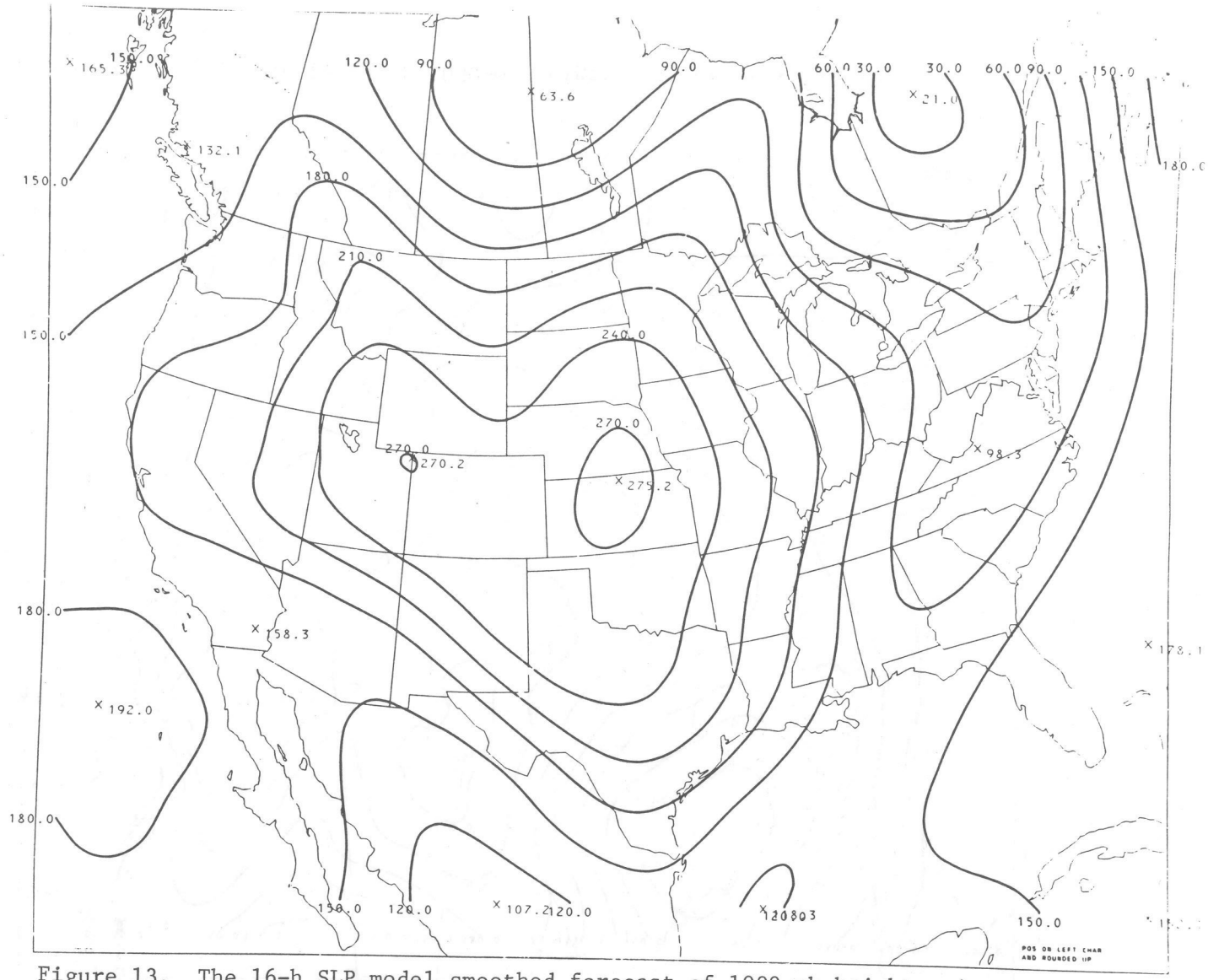

Figure 13. The 16-h SLP model smoothed forecast of 1000-mb heights, in meters, valid at 0000 GMT, March 11, 1979.

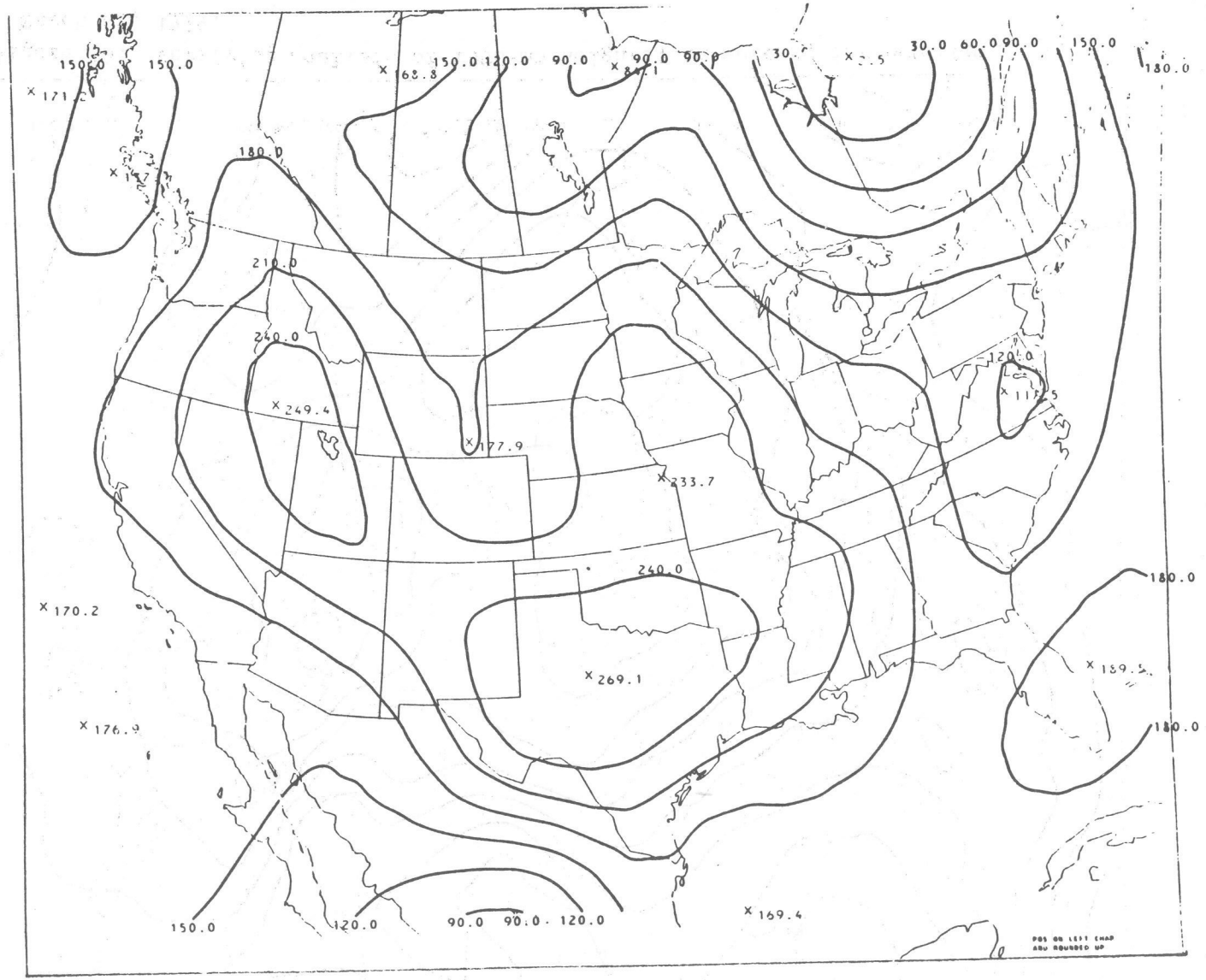

Figure 14. The 24-h LFM forecast of 1000-mb heights, in meters, valid at 0000 GMT, March 11, 1979.

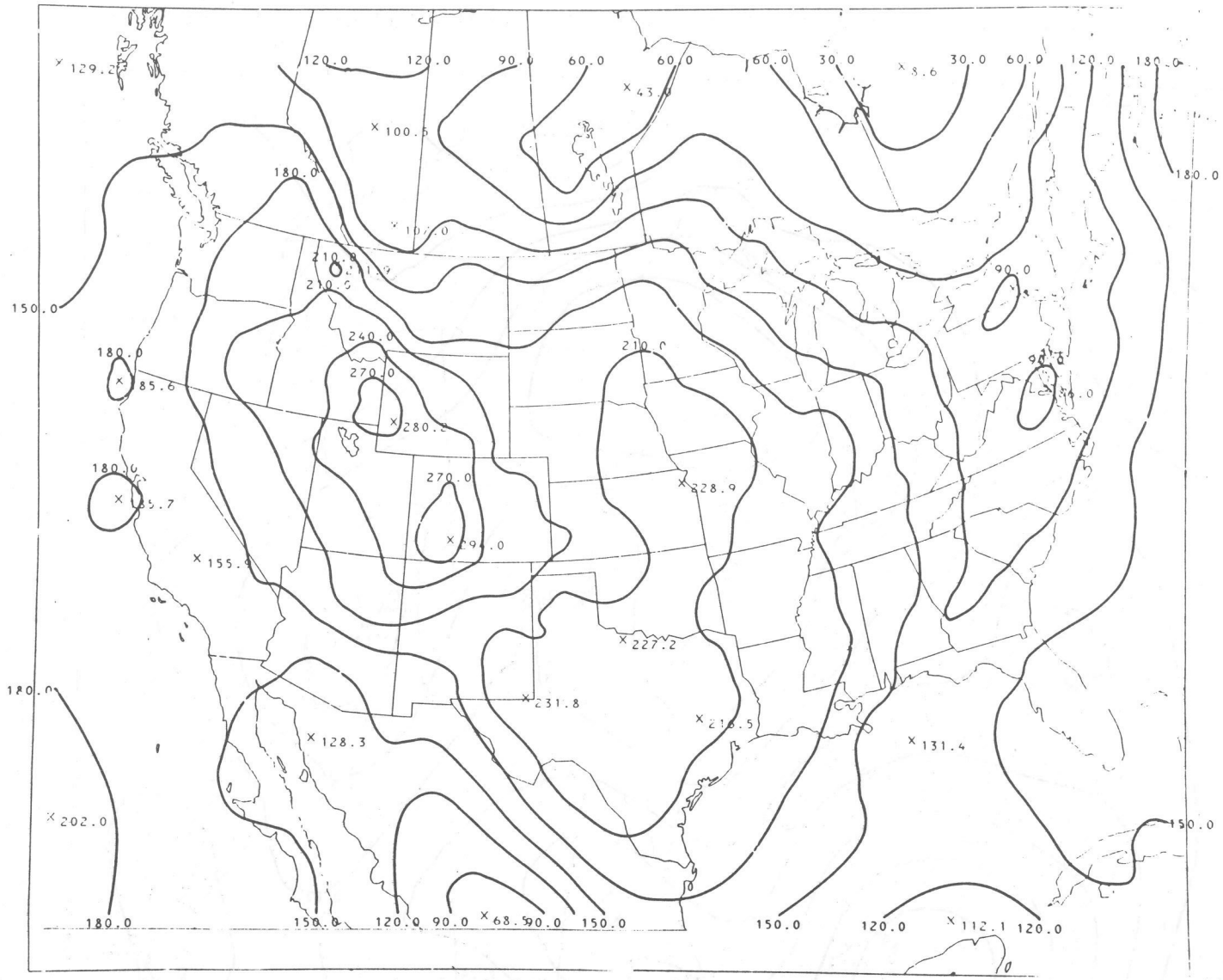

Figure 15. Verifying analysis of 1000-mb heights, in meters, for 0000 GMT, March 11, 1979.

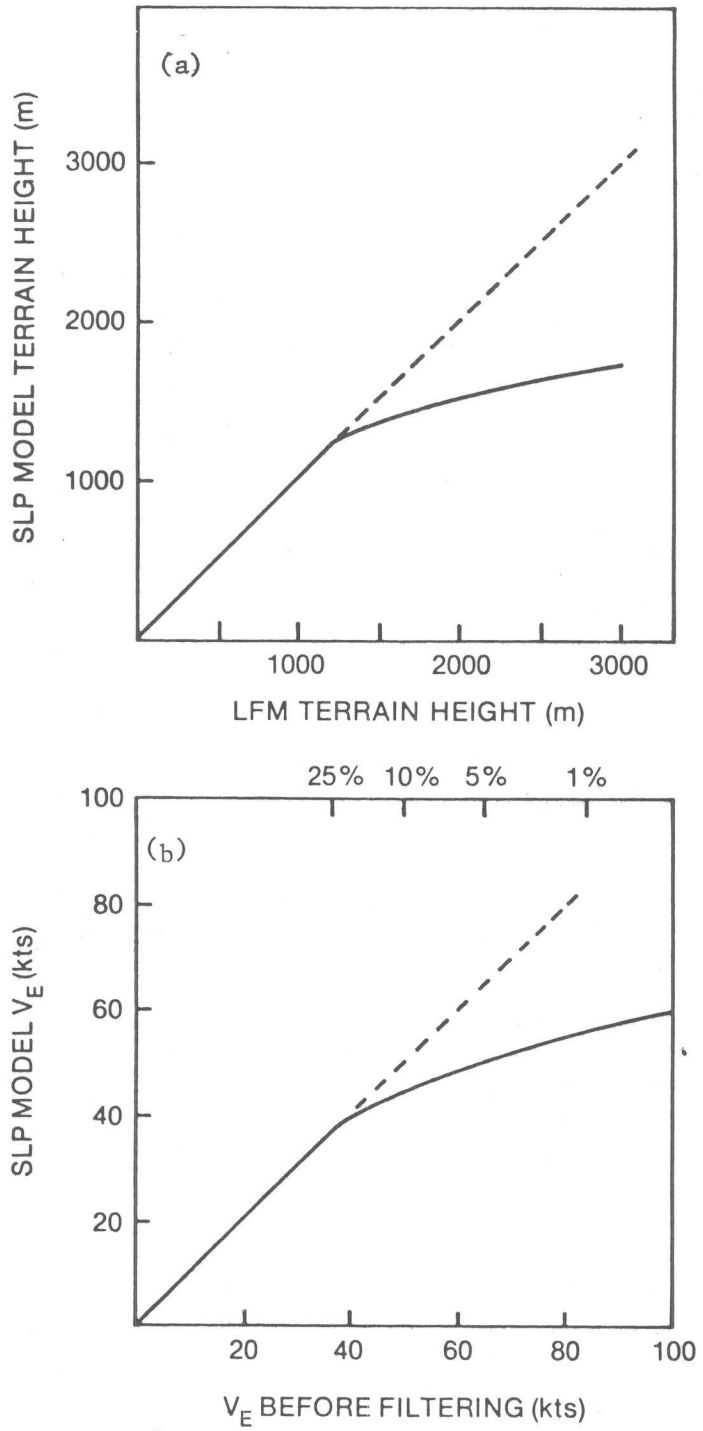

Figure 16. Filtered (solid) and unfiltered (dashed) terrain height (a) and advecting wind (b). Numbers at the top of b indicate the percentage of gridpoints above given wind speeds in the 16 sample predictions from the winter of 1979.

(Continued from inside front cover)

NOAA Technical Memorandums

NWS TDL 39 Computer Prediction of Precipitation Probability for 108 Cities in the United States. William H. Klein, February 1971, 32 pp. (COM-71-00249)

NWS TDL 40 Wave Climatology for the Great Lakes. N. A. Pore, J. M. McClelland, C. S. Barrientos, and W. E. Kennedy, February 1971, 61 pp. (COM-71-00368)

NWS TDL 41 Twice-Daily Mean Monthly Heights in the Troposphere Over North America and Vicinity. August F. Korte, June 1971, 31 pp. (COM-71-00826)

NWS TDL 42 Some Experiments With a Fine-Mesh 500-Millibar Barotropic Model. Robert J. Bermowitz, August 1971, 20 pp. (COM-71-00958)

NWS TDL 43 Air-Sea Energy Exchange in Lagrangian Temperature and Dew Point Forecasts. Ronald M. Reap, October 1971, 23 pp. (COM-71-01112)

NWS TDL 44 Use of Surface Observations in Boundary-Layer Analysis. H. Michael Mogil and William D. Bonner, March 1972, 16 pp. (COM-72-10641)

NWS TDL 45 The Use of Model Output Statistics (MOS) To Estimate Daily Maximum Temperatures. John R. Annett, Harry R. Glahn, and Dale A. Lowry, March 1972, 14 pp. (COM-72-10753)

NWS TDL 46 SPLASH (Special Program To List Amplitudes of Surges From Hurricanes): I. Landfall Storms. Chester P. Jelesnianski, April 1972. 52 pp. (COM-72-10807)

NWS TDL 47 Mean Diurnal and Monthly Height Changes in the Troposphere Over North America and Vicinity. August F. Korte and DeVer Colson, August 1972, 30 pp. (COM-72-11132)

NWS TDL 48 Synoptic Climatological Studies of Precipitation in the Plateau States From 850-, 700-, and 500-Millibar Lows During Spring. August F. Korte, Donald L. Jorgensen, and William H. Klein, August 1972, 130 pp. (COM-73-10069)

NWS TDL 49 Synoptic Climatological Studies of Precipitation in the Plateau States From 850-Millibar Lows During Fall. August F. Korte and DeVer Colson, August 1972, 56 pp. (COM-74-10464)

NWS TDL 50 Forecasting Extratropical Storm Surges For the Northeast Coast of the United States. N. Arthur Pore, William S. Richardson, and Herman P. Perrotti, January 1974, 70 pp. (COM-74-10719)

NWS TDL 51 Predicting the Conditional Probability of Frozen Precipitation. Harry R. Glahn and Joseph R. Bocchieri, March 1974, 33 pp. (COM-74-10909)

NWS TDL 52 SPLASH (Special Program to List Amplitudes of Surges From Hurricanes): Part Two. General Track and Variant Storm Conditions. Chester P. Jelesnianski, March 1974, 55 pp. (COM-74-10925)

NWS TDL 53 A Comparison Between the Single Station and Generalized Operator Techniques for Automated Prediction of Precipitation Probability. Joseph R. Bocchieri, September 1974, 20 pp. (COM-74-11763)

NWS TDL 54 Climatology of Lake Erie Storm Surges at Buffalo and Toledo. N. Arthur Pore, Herman P. Perrotti, and William S. Richardson, March 1975, 27 pp. (COM-75-10587)

NWS TDL 55 Dissipation, Dispersion and Difference Schemes. Paul E. Long, Jr., May 1975, 33 pp.(COM-75-10972)

NWS TDL 56 Some Physical and Numerical Aspects of Boundary Layer Modeling. Paul E. Long, Jr. and Wilson A. Shaffer, May 1975, 37 pp. (COM-75-10980)

NWS TDL 57 A Predictive Boundary Layer Model. Wilson A. Shaffer and Paul E. Long, Jr., May 1975, 44 pp. (PB-265-412)

NWS TDL 58 A Preliminary View of Storm Surges Before and After Storm Modifications for Alongshore-Moving Storms. Chester P. Jelesnianski and Celso S. Barrientos, October 1975, 16 pp. (PB-247-362)

NWS TDL 59 Assimilation of Surface, Upper Air, and Grid-Point Data in the Objective Analysis Procedure for a Three-Dimensional Trajectory Model. Ronald M. Reap, February 1976, 17 pp. (PB-256-082)

NWS TDL 60 Verification of Severe Local Storm Warnings Based on Radar Echo Characteristics. Donald S. Foster, June 1976, 9 pp. plus supplement. (PB-262-417)

NWS TDL 61 A Sheared Coordinate System for Storm Surge Equations of Motion With a Mildly Curved Coast. Chester P. Jelesnianski, July 1976, 52 pp. (PB-261-956)

NWS TDL 62 Automated Prediction of Thunderstorms and Severe Local Storms. Ronald M. Reap and Donald S. Foster, April 1977, 20 pp. (PB-268-035)

NWS TDL 63 Automated Great Lakes Wave Forecasts. N. Arthur Pore, February 1977, 13 pp. (PB-265-854)

NWS TDL 64 Operational System for Predicting Thunderstorms Two to Six Hours in Advance. Jerome P. Charba, March 1977, 24 pp. (PB-266-969)

NWS TDL 65 Operational System for Predicting Severe Local Storms Two to Six Hours in Advance. Jerome P. Charba, May 1977, 36 pp. (PB-271-147)

NWS TDL 66 The State of the Techniques Development Laboratory's Boundary Layer Model: May 24, 1977. P. E. Long, W. A. Shaffer, J. E. Kemper, and F. J. Hicks, April 1978, 58 pp. (PB-287-821)

NWS TDL 67 Computer Worded Public Weather Forecasts. Harry R. Glahn, November 1978, 25 pp. (PB-291-517)

NWS TDL 68 A Simple Soil Heat Flux Calculation for Numerical Models. Wilson A. Shaffer, May 1979, 16 pp. (PB-297-350)

NWS TDL 69 Comparison and Verification of Dynamical and Statistical Lake Erie Storm Surge Forecasts. William S. Richardson and David J. Schwab, November 1979, 20 pp. (PB 80 137797)